Published in final edited form as:
J Comp Neurol. 2011 October 1; 519(14): 2852–2869. doi:10.1002/cne.22661.

A Reassessment of Whether Cortical Motor Neurons Die Following Spinal Cord Injury

Jessica L. Nielson[1,2], **Melissa K. Strong**[1,2], and **Oswald Steward**[1,2,3,4,*]

[1]Reeve-Irvine Research Center, University of California at Irvine, Irvine, California 92697

[2]Department of Anatomy & Neurobiology, University of California at Irvine, Irvine, California 92697

[3]Department of Neurobiology & Behavior, University of California at Irvine, Irvine, California 92697

[4]Department of Neurosurgery, University of California at Irvine, Irvine, California 92697

Abstract

Over the past century, the question of whether the cells of origin of the corticospinal tract (CST) die following spinal cord injury (SCI) has been debated. A recent study reported an approximately 20% loss of retrogradely labeled cortical motoneurons following damage to their axons resulting from SCI at T9 (Hains et al. [2003] J. Comp. Neurol. 462:328–341). In follow-up studies, however, we failed to find any evidence of loss of CST axons in the medullary pyramid, which must occur if CST neurons die. Here, we seek to resolve the discrepancy by re-evaluating possible loss of CST neurons using the same techniques as Hains et al. (quantitative analysis of retrograde labeling and staining for cell death markers including TUNEL and Hoechst labeling of the nuclei). Following either dorsal funiculus lesions at thoracic level 9 (T9) or lateral hemisection at cervical level 5 (C5), our results reveal no evidence for a loss of retrogradely labeled neurons and no evidence for TUNEL staining of axotomized cortical motoneurons. These results indicate that CST cell bodies do not undergo retrograde cell death following SCI, and therefore targeting such cell death is not a valid therapeutic target. J. Comp. Neurol. 519:2852–2869, 2011.

INDEXING TERMS

corticospinal tract; retrograde degeneration; cell death; retrograde labeling

Spinal cord injury (SCI) results in a loss of function below the site of injury due to a disruption of the axons that relay information between the brain and the spinal cord. There has been great interest in developing therapeutic interventions to promote axon regeneration at the lesion site (for review, see Thuret et al., 2006) in hopes of promoting functional recovery. Such therapies assume, however, that the cell bodies of damaged axons remain alive. If the cell body dies, the axon will die as well (Carlson et al., 2000, 2001) and therapeutic interventions to promote axon regeneration would be futile. Therefore, it is crucial to establish whether the cells of origin of pathways affected by SCI undergo retrograde cell death. Here, we focus on the corticospinal tract (CST), as this is the most prominent descending motor pathway (Kuypers, 1981; Porter and Lemon, 1993) and its

*CORRESPONDENCE TO: Oswald Steward, Ph. D., 1105 GNRF, 837 Health Sciences Dr., University of California at Irvine, Irvine, CA 92697. osteward@uci.edu.

damage accounts for the paralysis that occurs following injuries to the spinal cord in humans.

The question of whether the cells of origin of the CST degenerate after damage to their axons has been explored for a century with inconsistent results. All such studies have focused on the motor cortex itself, using a variety of measures including: quantification of cortical neuron numbers (Bonatz et al., 2000; Feringa and Vahlsing, 1985; Feringa et al., 1983; Giehl and Tetzlaff, 1996; Hains et al., 2003; Hammond et al., 1999; Klapka et al., 2005; Sasaki et al., 2006), activation of cell death markers (Hains et al., 2003; Lee et al., 2004; Sasaki et al., 2006), changes in gene expression (Higo et al., 2009; Kost-Mikucki and Oblinger, 1991; Kost and Oblinger, 1993; Mason et al., 2003; Mikucki and Oblinger, 1991), changes in cortical representation (Jurkiewicz et al., 2007; Mikulis et al., 2002; Schmidlin et al., 2004, 2005) or cortical volume and tractography (Wrigley et al., 2009), changes in motor responses after stimulation in the cortex (Piecharka et al., 2005; Schmidlin et al., 2005), cell shrinkage (Beaud et al., 2008; Brock et al., 2010; Ganchrow and Bernstein, 1985; Holmes and May, 1909; Kalil and Schneider, 1975; Merline and Kalil, 1990; Ramirez and Kalil, 1985; Tseng and Prince, 1996; Wannier et al., 2005), and chromatolysis (Barron and Dentinger, 1979; Holmes and May, 1909; Lassek, 1942; Levin and Bradford, 1938). A few studies have reported no response to injury (Crawley et al., 2004; Mason et al., 2003; McBride et al., 1990).

The question has been addressed in a wide range of animal models including rats (Barron et al., 1988; Bonatz et al., 2000; Brock et al., 2010; Feringa and Vahlsing, 1985; Feringa et al., 1983; Ganchrow and Bernstein, 1985; Giehl and Tetzlaff, 1996; Hains et al., 2003; Hammond et al., 1999; Klapka et al., 2005; Lee et al., 2004; Mason et al., 2003; McBride et al., 1990; Piecharka et al., 2005; Sasaki et al., 2006; Tseng and Prince, 1996), hamsters (Kalil and Schneider, 1975; Kost-Mikucki and Oblinger, 1991; Kost and Oblinger, 1993; Merline and Kalil, 1990; Mikucki and Oblinger, 1991; Ramirez and Kalil, 1985), cats (Barron and Dentinger, 1979), dogs (Holmes and May, 1909), monkeys (Beaud et al., 2008; Brock et al., 2010; Higo et al., 2009; Holmes and May, 1909; Lassek, 1942; Levin and Bradford, 1938; Schmidlin et al., 2005; Schmidlin et al., 2004; Wannier et al., 2005), and humans (Crawley et al., 2004; Holmes and May, 1909; Jurkiewicz et al., 2007; Mikulis et al., 2002; Wrigley et al., 2009).

One noteworthy study among these previous reports seemed to provide compelling evidence that about 20% of the total CST cell bodies undergo retrograde cell death following injury to their axons from a T9 level SCI (Hains et al., 2003). The evidence was based on decreases in the number of retrogradely labeled CST neurons over time and appearance of cell death markers. Quantitative analyses indicated substantial CST neuron loss between 1 and 4 weeks post injury, suggesting that there is a short window of time available to intervene therapeutically to prevent cell death that would otherwise occur. In follow-up studies, however, we failed to find any evidence of loss of CST axons in the medullary pyramid, which must occur if CST neurons die (Nielson et al., 2010). Accordingly, here we reassess whether there is retrograde degeneration of CST neurons following SCI using the same methods used by Hains et al. We report that there is no loss of retrogradely labeled CST neurons following damage to CST axons in the spinal cord or evidence of activation of cell death markers following either T9 dorsal funiculus lesions or C5 hemisections.

MATERIALS AND METHODS

Animal use and care

All procedures were approved by the Institutional Animal Care and Use Committee (IACUC) at the University of California, Irvine in compliance with the National Institute of

Health guidelines. All animals used for this study were Sprague-Dawley outbred rats (Harlan Laboratories, San Diego, CA), maintained on a 12-hour light/dark cycle at 25°C. For surgery, rats were anesthetized with an intraperitoneal (i.p.) injection of ketamine and xylazine (100 mg/kg and 10 mg/kg, respectively; Western Medical Supply, Arcadia, CA). Postoperatively, rats received subcutaneous injections of 10 ml of 0.9% saline, 0.5 mg/kg Baytril (Bayer, Shawnee Mission, KS), and 0.01 mg/kg buprenorphine, and were kept warm on an isothermic pad until mobile and alert. Following injury, rats received saline and Baytril for up to 10 days post injury or until rats were euthanized. Buprenorphine was given for 7 days post injury. For rats with SCIs, bladders were manually expressed twice per day for the duration of the experiments. Some of the rats included here were also used for our previous study of CST axons in the medullary pyramid (Nielson et al., 2010), as further detailed below.

Injury paradigms

T9 dorsal funiculus lesion—In the first analysis, we used exactly the same procedures as Hains et al. (2003). Young male rats (150–175g at time of surgery) received a dorsal funiculus lesion (DF) at thoracic vertebral level 9 (T9), using ophthalmic microscissors (World Precision Instruments, Sarasota, FL, 7 cm long, curved 3-mm blades, 0.1-mm tips). These rats were also used in a previous study to assess degeneration of the CST in the medullary pyramid (Nielson et al., 2010). This injury paradigm bilaterally transects the dorsal CST (Fig. 1A) as described previously (Hains et al., 2003). During the surgery, the completeness of the injury was verified by using an operating microscope. Immediately after the lesion was completed, a 0.5 × 0.5 × 0.5-mm piece of Gelfoam (Pfizer, Groton, CT) impregnated with 5 μl of 4% (w/v in 0.9% saline) Fluoro-Gold (FG) was placed into the injury site, the muscles were sutured in layers, and the skin was closed with wound clips. DF lesions cause paralysis of the hindlimbs, and only transient bladder impairment during the first day following surgery, and did not affect normal eating, drinking, or grooming. Rats were allowed to survive for either 1 (n = 8) or 4 (n = 5) weeks following injury.

C5 lateral hemisection lesion—To assess possible retrograde changes due to lesions at a site relatively proximal to the cells of origin in the cortex, adult female rats (225–250 g at time of surgery) received a right lateral hemisection lesion (Hx) at cervical vertebral level 5 (C5) by using a Moria microknife, (catalog #7040A, Fine Science Tools, Foster City, CA). Data from these rats were also included in a previous study assessing CST axon degeneration in the medullary pyramid (Nielson et al., 2010). This injury paradigm unilaterally transects the crossed dorsal and dorsolateral and uncrossed ventral components of the CST (Fig. 1B) as described previously (Anderson et al., 2005). During surgery, the completeness of the injury was verified by using an operating microscope. As above, Gelfoam impregnated with FG was placed into the injury site, the muscles were sutured in layers, and the skin was closed with wound clips. C5 hemisections cause paralysis of the forearm and paw ipsilateral to the injury, with partial ipsilateral hindlimb paralysis, and transient bladder impairment for the first day following surgery. Eating and drinking were not impaired; however, grooming was predominantly with the left forelimb.

Rats were allowed to survive for either 1 week (n = 8) or 3 weeks (n = 5) following injury. This injury time point of 3 weeks was used, rather than 4 weeks as with the T9 paradigm, because some of the rats were from a previous study that assessed CST axons in the medullary pyramid at 3 weeks post hemisection (Nielson et al., 2010), so the additional rats prepared for the present study for the analysis of retrograde labeling were also killed at 3 weeks.

Cell death histology controls

Adult female Sprague-Dawley rats received subcutaneous injections of kainic acid (KA) (Sigma-Aldrich, St. Louis, MO) to induce seizures (Ben-Ari, 1985; Ben-Ari et al., 1980; Pisa et al., 1980; Sperk et al., 1983) and excitotoxic cell death (Ben-Ari, 1985; Ben-Ari et al., 1980; Sperk et al., 1983). Animals received repeated KA injections at a dose of 5 mg/kg until they reached a stage 5 seizure (Racine, 1972). Animals were killed humanely 3 days following injections (n = 2)

Perfusions

At the end of each experiment, animals received an i.p. injection of Euthasol (195 mg/ml pentobarbital sodium and 25 mg/ml phenytoin sodium; Delmarva Laboratories, Richmond, VA) and were transcardially perfused with 4% paraformaldehyde in 0.1 M phosphate-buffered saline (PBS), pH 7.4.

Histology

Brains and spinal cords were dissected and postfixed in 4% paraformaldehyde in 0.1 M PBS, pH 7.4. Forebrains and spinal cords were cryoprotected in 30% and 27% sucrose, respectively, frozen in TissueTek O.C.T.™ (VWR International, West Chester, PA), and stored at −80°C until they were sectioned.

Sectioning—Frozen brains and spinal cords were sectioned into 20-μm sections on a MICROM HM505 NP Series cryostat set at −20°C. Brains were sectioned coronally maintaining serial order, and sections were stored in PBS with 0.02% sodium azide (PBSA) in sterile 48-well plates, protected from light at 4°C until processing. Spinal cords were sectioned from segments spanning 8 mm rostral and caudal from the injury site. Spinal cords from rats that received T9 DF lesions were sectioned in the sagittal plane, whereas spinal cords from rats that received C5 hemisections were sectioned in the horizontal plane. Sagittal sections allow a more precise assessment of the depth of the T9 DF lesions and the degree to which the lesions destroy the main CST in the dorsal column. Horizontal sections allow a more precise assessment of whether lateral hemisection lesions extend to the midline to completely transect the main CST. Additional blocks caudal to the lesion site were sectioned in the coronal plane for assessment of spared CST fibers below the level of the injury. Sections were either directly mounted onto Fisherbrand Superfrost Plus glass slides (Fisher Scientific, Pittsburgh, PA) and allowed to dry overnight at room temperature, or maintained in serial order and stored in PBSA in 96-well plates and stored at 4°C. Sections on slides were either stained immediately, or stored at −80°C until stained for lesion verification and spared CST fibers.

Lesion verification—To reconstruct lesion sites, sections taken at 100-μm intervals (one in five) were mounted in serial order and stained for hemotoxylin and eosin (H&E). Slides were washed in PBS 3× 5 minutes each, then dehydrated in increasing concentrations of ethanol for 2 minutes each (70%, 95%, 100%, 100%), defatted in xylene for 5 minutes, and rehydrated in decreasing concentrations of ethanol for 2 minutes each (100%, 100%, 95%, 70%). Slides were then rinsed in tap water twice, stained with hematoxylin for 5 minutes, rinsed in tap water, dipped in acid alcohol, rinsed in tap water, dipped several times in ammonia water, and rinsed in tap water. Slides were then rinsed in 95% ethanol for 2 minutes, and stained with eosin for 15 seconds, dehydrated in 95% and 100% ethanol for 2 minutes each, defatted in xylenes 3 times for 3 minutes each, then coverslipped with DPX mounting media (Sigma-Aldrich), and viewed under a brightfield microscope.

To determine the overall extent of the lesions, a reconstruction of the area of the damage to the spinal cord was performed. The sections were viewed under the microscope in serial

order either from left to right in sagittal sections (T9 DF, Fig. 1C), or dorsal to ventral in horizontal sections (C5 Hx, Fig. 1D). Each section was assessed for damage to the white and gray matter, and the area of damage was estimated on a schematic cross section of the spinal cord, which was divided up into 100-μm intervals (Fig. 1E). The schematic in Figure 1 illustrates reconstructions of sagittal sections for the cases with T9 DF lesions and horizontal sections for the cases with C5 lateral hemisections. After all serial sections were assessed throughout the lesion, the reconstructed images were overlaid for each paradigm/time point by using Adobe Photoshop CS3 (San Jose, CA) (Fig. 1F,G for T9 DF; for C5 Hx see Nielson et al., 2010). The images were then multiplied together to show the variability in the lesions across cases (Fig. 1, gray scale) to show the average lesion size produced by their respective injury paradigm (Fig. 1A,B).

Completeness of the lesions was determined for the sagittal sections by assessing whether the lesion extended ventrally to include the ventral part of the dorsal column that contains the dorsal CST and the extent to which the lesions extended laterally into the dorsal horn. The same basic strategy was used to reconstruct C5 hemisections. In this case, we assessed whether the lesions extended to the midline or beyond at the different dorsoventral levels represented in the horizontal sections and the degree of sparing of tissue ventral or dorsal to the central canal. Only cases that completely ablated the dorsal CST (either bilaterally or unilaterally, for T9 and C5, respectively) were included in the quantitative analyses.

Histological assessment of spared CST fibers—Segments of the spinal cord caudal to the lesion site were assessed for spared CST fibers by immunostaining for the γ subunit of protein kinase C (PKCγ; Santa Cruz Biotechnology, Santa Cruz, CA, sc-211, lot # E-10-10; see below for information regarding the antibody). When used for immunocytochemistry, the antibody stains CST axons in the dorsal column (Akinori, 1998; Mori et al., 1990), and has been used in previous studies for assessment of spared CST fibers following SCI (Bradbury et al., 2002; Starkey et al., 2005).

Slide-mounted sections were incubated in 10% normal goat serum (Vector, Burlingame, CA) in PBS for 30 minutes at room temperature, and then in the primary antibody PKCγ (1:500 dilution in 0.1% sodium azide, 0.2% Triton X-100 in PBS) overnight at room temperature. Sections were washed 3 times in PBS for 5 minutes each, and then incubated in the secondary antibody Alexa Fluor 488 goat anti-rabbit IgG (Molecular Probes, Eugene, OR; 1:200 dilution in 0.1% sodium azide, 0.2% Triton X-100 in PBS) for 4 hours at room temperature, protected from light. Sections were rinsed in three washes of PBS and coverslipped with Vectashield mounting medium (Vector), sealed with nail polish, and visualized with a fluorescence microscope under the NB channel (excitation 470 nm, emission 515 nm).

Quantification of retrogradely labeled cells

For the rats that received DF lesions, coronal sections through the brain were mounted onto Fisherbrand Superfrost Plus microscope slides, and FG-labeled cell bodies were stereologically quantified. Pairs of adjacent sections (i.e., sections 1 and 2, 11 and 12, 21 and 22, etc.) taken at 200-μm intervals through the entire sensorimotor cortex (Bregma −4.0 mm to +4.0 mm; Paxinos, 1998) were used for unbiased sampling by using the physical dissector method. This counting method corrects for double counting of cells present in both reference and look-up sections. Photomicrographs were taken of each section in layer V of the sensorimotor cortex where FG-labeled cells were located by using the UV channel (excitation 360 nm, emission 420 nm). To avoid fading of FG fluorescence, once the labeled cells were in focus, the image was immediately captured and the shutter was closed to preserve fluorescence intensity. Images from adjacent sections were overlaid by using

Adobe Photoshop CS3 to align the sections. One section was designated the reference and the other the look-up, and cells were counted only if they were seen in one section and not the other (per the physical dissector). The total number of labeled cells in each hemisphere was estimated as follows: total cells = [(section thickness × section frequency) × (sum of cells counted)]/section thickness, where section thickness is 20 μm, section frequency is 200 μm, and the sum of the cells counted is the sum of cells counted in all sections sampled.

Assessment of cell atrophy

Stereological assessments of the size of retrogradely labeled neurons were carried out on sections that were immunostained by using an antibody to FG (Fluorochrome, Denver, CO; antibody to Fluoro-Gold, lot #1-7-09;see below for information regarding the antibody). Immunostaining for FG was used because FG fluorescence fades too quickly to measure cell size under the microscope. For immunostaining tissue sections, the antibody was used at a dilution of 1:60,000 combined with a peroxidase/diaminobenzidine (DAB) reaction to visualize cells under brightfield illumination (Akhavan et al., 2006).

Stereological measurements of the size of FG-labeled neurons were carried out in sections at approximately −0.2 mm from Bregma. This is the region in which Hains et al. (2003) report staining for cell death markers following SCI. Systematic random sampling with the fractionator technique was used to sample the FG-labeled cells in the cortex using the Stereo Investigator system (Micro-BrightField, Williston,VT; version 7.003 software; MBFBio-science). The area of the cortex containing the FG-labeled cells was traced to define the sampling area. In order to obtain a coefficient of error of <5%, each fractionator box was sized to 50 × 50 μm, with approximately 50 sampling sites throughout the cell layer. Cell size area was measured by using the nucleator probe (Gundersen,1988), with six intersecting lines used to calculate the area of each cell. Only cells that displayed a prominent nucleolus that came into focus within the middle 75% of the tissue thickness were measured.

TUNEL detection of apoptosis

To determine whether CST cell bodies exhibited molecular signs of apoptosis following SCI, sections from selected brains from T9 DF (1 week and 4 weeks) and C5 Hx (1 week) were assessed with the terminal deoxynu-cleotidyl transferase dUTP nick end labeling (TUNEL) assay (TUNEL in situ cell death labeling kit, Roche Applied Science, Indianapolis, IN). For TUNEL staining, sections were selected from the area with the highest density of FG-labeled neurons (about 0.2 mm posterior to Bregma). Mounted sections were first imaged under the UV channel for FG-labeled cells. Slides were then fixed with 4% paraformaldehyde for 20 minutes at room temperature, and then washed in PBS for 30 minutes. Sections were then permeabilized by microwave irradiation in 0.1 M sodium citrate for 5 minutes and rinsed twice in PBS.

The area around the sections was dried and each section was covered with 50 μl of TUNEL reaction mixture containing TdT and rhodamine-dUTP (in 200 mM cacodylic acid, 200 mM KCl, 1 mM EDTA, 4 mM -mercaptoethanol, 25 mM Tris-HCl, 1 mM $CoCl_2$, 0.25 mg/ml bovine serum albumin [BSA], and 50% glycerin), covered with Parafilm and incubated in a humidified chamber for 1 hour at 37°C, protected from light. Slides were rinsed 3 times in PBS and then immediately imaged on the microscope for TUNEL labeling under the NB channel (excitation 450–500 nm, emission 515–565 nm). Sections were processed alongside both positive and negative controls. Positive controls consisted of sections from KA-injected rats as well as sections pretreated with DNase I (1 μl/ml in 50 mM Tris-HCl, pH 7.5, 10 mM $MgCl_2$, 1 mg/ml BSA in double-distilled water) for 10 minutes at 37°C. Negative controls consisted of both uninjured animals and sections that did not receive TdT enzyme in the TUNEL reaction mixture.

Nuclear stain with Hoechst

Sections from T9 DF (1 and 4 weeks), C5 Hx (1 week), and uninjured FG-injected controls at T9 were stained with the nuclear marker Hoechst 33258 (Invitrogen, Carlsbad, CA) to assess the heath of the nuclei in FG-labeled cells. Mounted sections were washed 3 times for 5 minutes each in PBS (1X), then for 5 minutes in 1:10,000 dilution in 1X PBS, and rinsed again three times in 1X PBS at 5 minutes each. Sections were allowed to air dry and were coverslipped and viewed under the UV fluorescence channel for Hoechst labeling (excitation 360 nm, emission 420 nm). The UV channel also reveals FG and in sections stained with Hoechst, Hoechst staining is blue, whereas the FG labeling appears orange and therefore nuclei can be identified within the FG-labeled cells without further processing.

Antibodies

The antibody against PKCγ was produced in rabbit by immunization with a synthetic peptide corresponding to residues 679–697 of mouse PKCγ (DFVHPDARSPTSP VPVPVM), summarized in Table 1. Previous studies have shown that this antibody labels two closely spaced bands in Western blots prepared from rat cerebellum and neocortex with an approximate molecular weight of 80 kDa (Cardell et al., 1998). Because the antibody is used here as a marker for CST axons in the dorsal column, the key validation is the disappearance of immunostaining following lesions that destroy the CST (see Results).

The antibody against FG was produced in rabbits following immunization by FG itself (Table 1). Specificity is demonstrated by the fact that the pattern of immunostaining of retrogradely labeled neurons corresponds to the pattern seen when FG is directly visualized by fluorescence (Bezdudnaya and Keller, 2008; Chomsung et al., 2008; Lee et al., 2009; Masterson et al., 2009).

Area and volume measurements of regions that contain FG-labeled cells

Low-magnification images (4×) of sections throughout the left cortex were used to assess the area and volume of the region containing retrogradely labeled cells. Every 40th image was photographed and tiled to reconstruct each section to illustrate the rostrocaudal distribution of retrogradely labeled neurons. The area of the region containing the labeled cell bodies in each section was analyzed by using ImageJ (image processing and analysis software, National Institutes of Health, Bethesda, MD) by calibrating the pixel/micron ratio, and then tracing the region of the labeled cell bodies in the cortex for each side. The volume of the region was then calculated across sections by the following equation: $[\sum (A \times t)_N]$ = summation (∑) of the area (A) for each section multiplied by the distance between each section (t = 800 μm) for the set number of sections (N) with retrogradely labeled neurons.

Microscopy and image adjustment

Images were captured on an Olympus AX-80 microscope (Olympus, Center Valley, PA) by using MagnaFire SP2.1B software (Optronics Software, Goleta, CA). Fluorescence images in Figures 3 and 5 were composed of multiple low-magnification images that were tiled together by using the overlay function in Adobe Photoshop CS3. Due to variations in background brightness, the paintbrush tool was used to even out the color distribution of the background around the tissue. For Figure 9, images were color matched to the uninjured control (Fig. 9A), by using the image adjustment:match color function in Adobe Photoshop CS3.

Statistical analysis

Data were analyzed for statistical significance by using either a t-test for total cell counts and cell size/area measurements, a one-way analysis of variance (ANOVA) for the FG

detection method, or a two-way ANOVA for rostrocaudal cell counts with post hoc analyses with the Bonferroni Multiple Comparison Test. Graphs are plotted as the average, with the error bars representing the standard deviation.

RESULTS

Lesion verification

Examination of serial sagittal sections through the T9 lesion site revealed that all lesions ablated the dorsal column bilaterally and extended ventrally into the gray matter past the central canal, and laterally into the dorsal horns (Fig. 1A) at both 1 (Fig. 1F) and 4 weeks (Fig. 1G). Examination of serial horizontal sections through C5 hemisections revealed that in all cases killed 1 week post C5 hemisection, the crossed dorsal CST was completely transected (Fig. 1B). In some cases, the lesion extended over the midline to affect the dorsal CST on the contralateral side, and in some cases the lesion was incomplete laterally, sparing the dorsolateral CST (for lesion reconstructions, refer to Nielson et al., 2010) (Fig. 1B,D).

In three of five of the cases killed 3 weeks post injury, hemisections were incomplete, sparing a portion of the dorsal CST. Cases with incomplete lesions of the dorsal CST were not included in the analysis of FG-labeled cells. Because there were only two cases with complete lesions at 3 weeks post injury, quantitative comparisons of numbers of labeled cells 1 vs. 3 weeks post injury were not feasible, so cell counts and measurements were not carried out.

Confirmation of lesions to the CST

To confirm transection of CST axons, cross sections taken caudal to the injury were immunostained by using a polyclonal antibody to PCKγ, which labels CST axons in the DF (Fig. 2A). With complete DF lesions, immunostained CST axons weree no longer present in the DF caudal to the lesion (Fig. 2C). Incomplete lesions were revealed by partial preservation of immunostaining caudal to the lesion (Fig. 2B). Following lateral hemisections, immunostaining in the area of the CST was lost ipsilateral to the lesion and preserved on the contralateral side (Fig. 2D). As an aside, it is noteworthy that there was increased immunostaining of interneurons of lamina II in the dorsal horn gray matter compared with uninjured controls; this has previously been reported in studies of neuropathic pain following injury (Basbaum, 1999; Martin et al., 1999; Neumann et al., 2008). Cases with spared CST immunostaining in the DF were excluded from the quantitative analysis of retrogradely labeled cells, described below.

No decrease in the number of retrogradely labeled cells over time following DF lesions at T9

FG injections at T9 led to retrograde labeling of cell bodies in the somatosensory and motor cortex (Bregma 1.8 mm to −3.8 mm). The distribution of labeled neurons was similar on the two sides of the brain, so only the left cortex is illustrated (Fig. 3). Retrogradely labeled neurons were found from approximately Bregma 1.8 mm to −3.8 mm. No labeled neurons were seen in the more rostral areas of the prefrontal and cingulate cortex, or in the parietal cortex where retrograde labeling was observed following FG injections at C5 (see below). The pattern of labeling was qualitatively similar at 1 and 4 weeks post injury (Fig. 4A vs. B). Counts of retrogradely labeled neurons with the physical dissector method at 1 and 4 weeks following DF lesions are shown as mean counts per section throughout the rostrocaudal extent of the sensorimotor cortex (Fig. 4C), and as the total number of cells estimated based on the sum of the mean counts per section, factoring in the distance between each section (Fig. 4D).

Rostrocaudal counts of retrogradely labeled cells following DF lesions at T9 revealed no significant differences in cell numbers at 1 vs. 4 weeks post injury. Indeed, the means were almost identical. The counts revealed a bell-shaped curve of distribution throughout the rostrocaudal axis, spanning from 2.8 mm to −2.0 mm from Bregma, with the peak number of cells at 0.4 mm from Bregma. At this peak, the mean cell count 1 week following T9 DF was 148 ± 15 cells vs. 140 ± 14 cells at 4 weeks following injury (Fig. 4C). The total number of retrogradely labeled CST neurons was about 11% less at 4 weeks vs. 1 week post injury (20,611 ± 2,065 at 4 weeks vs. 23,740 ± 3,969 at 1 week), but this difference was not statistically significant ($P = 0.13$, Fig. 4D).

There was some variability in the size of the lesions resulting from T9 DF injuries (Fig. 1), and some variability in the number of retrogradely labeled neurons across cases. Accordingly, it was of interest to determine whether there was a relationship between lesion size and the number of retrogradely labeled neurons. Scatter plots of lesion size vs. number of retrogradely labeled neurons (Fig. 4E) revealed no significant correlation between these variables either at 1 ($R^2 = 0.1775$; $P = 0.30$) or 4 weeks ($R^2 = 0.0480$; $P = 0.7232$) following injury. Thus, in cases with complete lesions of the DF, the amount of additional damage to the spinal cord does not significantly affect the degree of retrograde labeling of CST neurons.

It is noteworthy that the absolute counts are substantially higher than the counts in Hains et al. with the same injury paradigm, animal model, and labeling technique. In the data of Hains et al. there were only 52 cells at the peak rostrocaudal location in the cortex (Bregma −0.2 mm) 1 week following injury, and 30 cells at 4 weeks. Additionally, their total cell counts were substantially less, with only 6,560 cells counted at the 1-week time point, and 3,000 total cells at 4 weeks (Hains et al., 2003). In this regard, we counted all neurons in which there was detectable labeling, whereas Hains et al. apparently only counted neurons with “strong signal,” which could account for the differences in total numbers of neurons counted. This would not, however, account for decreases in the numbers of labeled neurons over time unless there was a time-dependent decrease in fluorescence labeling intensity so that lightly labeled neurons fell below their counting threshold. In this regard, there were differences in fluorescence labeling intensity between cases, but the differences were not systematically related to time post injury.

Survival of CST neurons after lateral hemisections at C5

Our previous study that evaluated CST axon integrity in the medullary pyramid after SCI (Nielson et al., 2010) also assessed the consequences of lateral hemisections at C5. Lesions at C5 are more proximal to the cells of origin, and we reasoned that such proximal axonal lesions might be more likely to induce retrograde cell death. The other advantage of a lateral hemisection injury is that it primarily affects axons from one side of the cortex, allowing comparisons of axotomized neurons in the cortex contralateral to the lesion with noninjured cells on the opposite side. Accordingly, we also assessed retrograde labeling following FG injections in rats that sustained C5 hemisections and stained tissue from animals with C5 hemisections for TUNEL and with Hoeschst.

Figure 5 illustrates an example of the distribution of retrogradely labeled neurons following C5 hemisections and FG injections. CST axons that project to thoracic and lumbar levels pass through cervical segments, so it is to be expected that injections of FG at C5 would label a larger number of CST neurons than injections at T9. Indeed, following FG injections at C5 retrogradely labeled neurons were found in the prefrontal, anterior cingulate (Bregma 4.2 mm to 3.4 mm), sensorimotor (Bregma 4.2 mm to −3.8 mm), and posterior parietal (Bregma − 1.4 mm to −2.2 mm) cortices (Fig. 5). This overall distribution of retrogradely labeled cells was similar to what has been reported previously following horseradish

peroxidase (HRP) injections at C5/6 in adult Long Evans rats (Miller, 1987). The overall volume of the cortex that contained labeled neurons and the overall number of labeled neurons was greater than following FG injections at T9 (Fig. 6C,D).

To document the differential distribution of retrogradely labeled neurons, one representative case per injury/ injection paradigm was reconstructed and assessed. FG injections at C5 resulted in peak area of labeling of CST neurons of 1.07×10^6 μm^2 1 mm rostral to Bregma (Fig. 6C) and a total volume throughout the entire cortex of 6.54×10^9 μm^3 (Fig. 6D). CST neurons in the cortex following thoracic labeling resulted in a peak area of 7.30×10^6 μm^2 6 mm caudal to Bregma (Fig. 6C) and a total volume throughout the cortex of 2.46×10^9 μm^3 (Fig. 6D). Therefore more rostral and caudal projecting corticospinal neurons are located in the more rostral and caudal regions of the cortex, respectively.

Evidence for atrophy of CST cell bodies following SCI

It was of interest to determine whether we could confirm previous reports of decreases in CST neuron size following SCI, indicative of retrograde atrophy (Brock et al., 2010; Holmes and May, 1909). To assess this, sections were immunostained for FG, because FG fluorescence fades during viewing under the microscope. In order to determine whether the antibody to FG detects all cells that contain FG, a quality control assay was performed to ensure that the same numbers of labeled cells were seen with fluorescence (Fig. 7A) vs. immunostaining (Fig. 7B). Sections were imaged for FG fluorescence, then processed for FG-Ab, and then images were taken of the immunostained sections. Counts revealed approximately the same number of neurons labeled by fluorescence vs. immunostaining (Fig. 7D). Therefore we felt confident using the FG antibody to assess atrophy by using Stereo Investigator, whereby the nucleator probe was used to measure cell area, including only cells displaying a prominent nucleolus (Fig. 7C).

Cell size measurements were carried out in seven rats killed 1 week post DF lesion and six rats killed 4 weeks post lesion. More animals were assessed here than for the fluorescent cell counts because not all cases had bright enough FG fluorescence to allow reliable cell counts at the magnifications used. Analysis of neuron size following immunostaining was done at high magnification, however, and fading of signal was not an issue. The comparisons (Fig. 7E) revealed that the average size of retrogradely labeled CST neurons was significantly smaller at 4 weeks post DF lesion (222.88 ± 72.01 μm^2) than at 1 week (255.00 ± 81.25 μm^2; $P = 0.003$). This is consistent with the interpretation that CST cell bodies do undergo retrograde atrophy as a result of SCI. However, there was no significant correlation between lesion size and neuron size either at 1 ($R^2 = 0.5114$; $P = 0.07$) or 4 weeks ($R^2 = 0.7230$; $P = 0.15$) following T9 DF lesions (Fig. 7F).

No evidence of apoptosis of CST cell bodies following SCI

Hains et al. also report that CST neurons display signs of apoptosis following T9 DF lesions as evidenced by DNA fragmentation (Walker et al., 1988), revealed by TUNEL staining (Gavrieli et al., 1992; Migheli et al., 1995). Indeed, Hains et al. report that approximately 40% of the FG-labeled CST neurons were TUNEL positive. Some CST neurons also displayed nuclear condensation as revealed by Hoechst staining, which is considered to be a sign of apoptosis.

Assessment of TUNEL staining in the FG-labeled cell bodies following T9 SCI revealed no evidence of DNA fragmentation (Fig. 8) or abnormal nuclear profiles (Fig. 9) that would suggest that these cells were undergoing apoptotic cell death. Positive controls for TUNEL included DNase I treatment (Fig. 8B), and parallel staining of sections from animals exhibiting excitotoxic cell death due to KA-induced seizures (Fig. 8A). There was no

evidence of TUNEL labeling in the cortex either 1 or 4 weeks following T9 DF lesions (Fig. 8G,I; FG-labeled cells are shown in Fig. 8F,H, respectively). Similarly, there was no evidence of abnormal or apoptotic nuclei when assessment was done with Hoechst either 1 week (Fig. 9C) or 4 weeks (Fig. 9D) following DF lesions at T9.

In keeping with the results following T9 DF lesions, retrogradely labeled CST neurons also did not exhibit TUNEL staining after C5 hemisections (Fig. 8E; FG-labeled cells are shown in Fig. 8D). Also, we did not detect CST neurons with abnormal or apoptotic nuclei when assessment was done with Hoechst (Fig. 9B). For comparison, Figure 9A illustrates uninjured retrogradely labeled CST neurons from the cortex ipsilateral to the C5 hemisection.

DISCUSSION

Here, we re-evaluated whether SCI and the resulting damage to CST axons causes retrograde degeneration of cortical motoneurons. A previous study reports a substantial loss of retrogradely labeled CST neurons following T9 SCI (Hains et al., 2003). Following identical lesions, and assessing with identical methods, we see no such loss. Hains et al. also report that a large number of CST neurons stain positively for TUNEL at 1 week post injury and exhibit nuclear changes consistent with apoptosis. Again, using identical methods, we see no such changes. We further explored whether signs of retrograde degeneration could be detected following injuries that were more proximal to the cell body, specifically following a lateral hemisection at C5, which also provides an internal control (cortical motoneurons ipsilateral to the hemisection, whose axons would not have been transected). Again, we found no evidence of apoptosis (no TUNEL-positive cortical motoneurons or neurons with abnormal nuclei). Our results do confirm previous reports of decreases in the size of CST neuron somata that may reflect retrograde atrophy. In what follows, we discuss possible experimental variables that might account for these discrepant results, and then the implications of our findings.

Can the discrepancy be explained by differences in methods?

Our goal here was to use the same injury models and methodology used by Hains et al. (2003), and then follow up with other injury models (C5 hemisection). We used rats of the same strain, age, and sex used by Hains, the same injury model (dorsal funiculus lesions), and the same retrograde tracing procedures.

One difference to be noted was the dosage of anesthetic used during surgical procedures. Higher dosages of ketamine (100 mg/kg) and xylazine (10 mg/kg) were used in the present study compared with the Hains et al. study (80/5 mg/kg, respectively). It is conceivable that the higher drug dose may have a neuroprotective effect. It has been shown previously that a ketamine/xylazine cocktail at the time of surgery promotes the survival of retinal ganglion cells after axotomy in rats (Ozden and Isenmann, 2004), compared with other commonly used anesthetics such as chloral hydrate (Isenmann et al., 1997; Ozden and Isenmann, 2004). However, in terms of the affects of different dosages of ketamine and/or xylazine on CST neurons, the predominant pattern in the literature does not suggest that this is an influential factor of cell survival. Ketamine doses of 50 mg/kg in rats (Brock et al., 2010), and 5 (Wannier et al., 2005) or 1 mg/kg in monkeys (Brock et al., 2010) show consistent findings with the present study in that CST neurons survive the injury, albeit in a shrunken/atrophied state (Brock et al., 2010; Wannier et al., 2005). These doses are considerably lower than those in the Hains et al. study, and yet still show cell survival. Therefore it is unlikely that the higher dose used in the present study is inducing a robust enough neuroprotective effect to reverse the retrograde cell death reported in the Hains et al. study.

In terms of the analyses, the only difference we can detect is our method of cell counting, in which we counted all neurons with fluorescent label. In contrast, Hains et al. describe a counting method in which neurons were counted only if they displayed “prominent nuclear profiles and strong signal.” Seemingly, these criteria would lead to the exclusion of neurons in which retrograde labeling was light. If there are decreases in fluorescence intensity over time following SCI, these criteria could result in fewer cells being counted even if the eliminated cells still exhibited fluorescent labeling. This difference in counting may account for the discrepancy between our results and those of Hains et al.

Discrepancy in TUNEL labeling between the two studies

Hains et al. also reported that a substantial percentage of cortical motoneurons exhibited TUNEL staining, and some exhibited nuclear fragmentation. DNA fragmentation is associated with apoptosis (Walker et al., 1988), and therefore its detection suggests that the cell is in fact dying. The reason for the absence of TUNEL labeling in our study cannot be explained by any methodological difference we can identify. Our positive controls revealed substantial numbers of TUNEL-positive neurons following KA-induced seizures, but no TUNEL-positive CST neurons were seen in tissue from SCI rats that were run in parallel. Thus, we have no satisfactory explanation for the discrepant results.

Significance of a lack of retrograde degeneration of cortical motoneurons

The present study, along with our study of CST axon numbers in the medullary pyramid (Nielson et al., 2010) provides compelling evidence that cell bodies of the CST in the cortex do not die following damage to their axons as a result of SCI. Although we only assessed cell loss out to 4 weeks post injury, our previous study assessing the axons of the CST in the medullary pyramid reported no degeneration or loss of axons, even up to 1 year following injury (Nielson et al., 2010).

One explanation for the lack of retrograde degeneration of CST neurons after SCI is the presence of sustaining collaterals rostral to the site of injury (Brodal et al., 1956; Broere, 1971; Rossi and Brodal, 1956; Shinoda et al., 1986). In addition, growth of new connections in the spinal cord following injury (Bareyre et al., 2004; Brosamle and Schwab, 1997; Maier et al., 2008; Rosenzweig et al., 2010) may enable CST neurons to survive.

The present study repeats the procedures and analyses carried out by Hains et al. (2003) and thus represents another in a series of recent replication studies carried out through a program established by the National Institute of Neurological Disorders and Stroke (NINDS; NINDS, 2008). Like several previous replication experiments (Pinzon et al., 2008; Steward et al., 2006, 2008), the present study fails to replicate the findings in the target articles. Other replication experiments were studies of treatments or interventions that had been reported to enhance neural sparing, regenerative growth, or recovery of function. Here, however, we fail to replicate a phenomenon.

Retrograde atrophy is consistent with the literature

Although there has been controversy and various outcomes reported in the literature regarding the fate of the CST neurons following axotomy, the most consistent outcome appears to be shrinkage and atrophy (Barron and Dentinger, 1979; Barron et al., 1988; Brock et al., 2010; Carter et al., 2008; Ganchrow and Bernstein, 1985; Holmes and May, 1909; Kalil and Schneider, 1975; Lassek, 1942; Merline and Kalil, 1990; Ramirez and Kalil, 1985; Tseng and Prince, 1996). The analyses in the present study are consistent with a modest but significant shrinkage of the cell bodies of CST neurons.

Atrophy likely reflects a decrease in neuronal metabolism and viability, and could contribute to regeneration failure and/or impaired function of surviving projections. In this way, retrograde atrophy may still represent an important target for therapy. In this regard, recent studies have shown that atrophy of cortical motoneurons can be prevented or reversed by treatment with brain-derived neurotrophic factor (BDNF) (Brock et al., 2010) in the same way that BDNF treatment reverses retrograde atrophy of neurons in the red nucleus (Kwon et al., 2007), even up to 1 year following SCI (Kwon et al., 2002). Other therapeutic interventions, such as treatment with anti-NogoA-antibody have not been successful at preventing this retrograde atrophy (Beaud et al., 2008), suggesting that there is room for improvement regarding this treatment strategy.

CONCLUSIONS

The continued survival of most, if not all, cortical motoneurons following SCI has important implications. As noted by Hains et al. (2003), if a significant number of CMNs did die, then this would be an important impediment to efforts to stimulate regeneration of their axons. Indeed, the Hains et al. article triggered subsequent studies that specifically cited the Hains et al. data as their rationale for exploring therapeutic interventions to prevent retrograde cell death (Sasaki et al., 2006, 2009). Our findings that the CST survives SCI, by assessing both the cell bodies in the cortex and the axons in the medullary pyramid, even up to 1 year following injury (Nielson et al., 2010), suggest that there is a significant therapeutic time frame available for boosting cell vitality and recovery of function.

Acknowledgments

Thanks to Aileen J. Anderson and Brian J. Cummings for use of Stereo Investigator, and to Kelli Sharp for technical assistance.

Grant sponsor: NIH; Grant number: NS047718 (to O.S.); Grant sponsor: the Roman Reed Spinal Cord Injury Research Fund of California; private donations to the Reeve-Irvine Research Center

LITERATURE CITED

Akhavan M, Hoang TX, Havton LA. Improved detection of fluorogold-labeled neurons in long-term studies. J Neurosci Methods. 2006; 152:156–162. [PubMed: 16246425]

Akinori M. Subspecies of protein kinase C in the rat spinal cord. Prog Neurobiol. 1998; 54:499–530. [PubMed: 9550189]

Anderson KD, Gunawan A, Steward O. Quantitative assessment of forelimb motor function after cervical spinal cord injury in rats: relationship to the corticospinal tract. Exp Neurol. 2005; 194:161–174. [PubMed: 15899253]

Bareyre FM, Kerschensteiner M, Raineteau O, Mettenleiter TC, Weinmann O, Schwab ME. The injured spinal cord spontaneously forms a new intraspinal circuit in adult rats. Nat Neurosci. 2004; 7:269–277. [PubMed: 14966523]

Barron KD, Dentinger MP. Cytologic observations on axotomized feline Betz cells. 1. Qualitative electron microscopic findings. J Neuropathol Exp Neurol. 1979; 38:128–151. [PubMed: 261986]

Barron KD, Dentinger MP, Popp AJ, Mankes R. Neurons of layer Vb of rat sensorimotor cortex atrophy but do not die after thoracic cord transection. J Neuropathol Exp Neurol. 1988; 47:62–74. [PubMed: 3275429]

Basbaum AI. Spinal mechanisms of acute and persistent pain. Reg Anesth Pain Med. 1999; 24:59–67. [PubMed: 9952097]

Beaud ML, Schmidlin E, Wannier T, Freund P, Bloch J, Mir A, Schwab ME, Rouiller EM. Anti-Nogo-A antibody treatment does not prevent cell body shrinkage in the motor cortex in adult monkeys subjected to unilateral cervical cord lesion. BMC Neurosci. 2008; 9:5. [PubMed: 18194520]

Ben-Ari Y. Limbic seizure and brain damage produced by kainic acid: mechanisms and relevance to human temporal lobe epilepsy. Neuroscience. 1985; 14:375–403. [PubMed: 2859548]

Ben-Ari Y, Tremblay E, Ottersen OP. Injections of kainic acid into the amygdaloid complex of the rat: an electro-graphic, clinical and histological study in relation to the pathology of epilepsy. Neuroscience. 1980; 5:515–528. [PubMed: 6892841]

Bezdudnaya T, Keller A. Laterodorsal nucleus of the thalamus: a processor of somatosensory inputs. J Comp Neurol. 2008; 507:1979–1989. [PubMed: 18273888]

Bonatz H, Rohrig S, Mestres P, Meyer M, Giehl KM. An axotomy model for the induction of death of rat and mouse corticospinal neurons in vivo. J Neurosci Methods. 2000; 100:105–115. [PubMed: 11040372]

Bradbury EJ, Moon LD, Popat RJ, King VR, Bennett GS, Patel PN, Fawcett JW, McMahon SB. Chondroitinase ABC promotes functional recovery after spinal cord injury. Nature. 2002; 416:636–640. [PubMed: 11948352]

Brock JH, Rosenzweig ES, Blesch A, Moseanko R, Havton LA, Edgerton VR, Tuszynski MH. Local and remote growth factor effects after primate spinal cord injury. J Neurosci. 2010; 30:9728–9737. [PubMed: 20660255]

Brodal A, Szabo T, Torvik A. Corticofugal fibers to sensory trigeminal nuclei and nucleus of solitary tract; an experimental study in the cat. J Comp Neurol. 1956; 106:527–555. [PubMed: 13416406]

Broere, G. Oegstgeest. The Netherlands: De Kempenaer; 1971. Corticofugal fibers in some mammals. An experimental study with special emphasis on the corticospinal system.

Brosamle C, Schwab ME. Cells of origin, course, and termination patterns of the ventral, uncrossed component of the mature rat corticospinal tract. J Comp Neurol. 1997; 386:293–303. [PubMed: 9295153]

Cardell M, Landsend AS, Eidet J, Wieloch T, Blackstad TW, Ottersen OP. High resolution immunogold analysis reveals distinct subcellular compartmentation of protein kinase C gamma and delta in rat Purkinje cells. Neuroscience. 1998; 82:709–725. [PubMed: 9483530]

Carlson J, Armstrong B, Switzer RC 3rd, Ellison G. Selective neurotoxic effects of nicotine on axons in fasciculus retroflexus further support evidence that this a weak link in brain across multiple drugs of abuse. Neuropharma-cology. 2000; 39:2792–2798.

Carlson J, Noguchi K, Ellison G. Nicotine produces selective degeneration in the medial habenula and fasciculus retroflexus. Brain Res. 2001; 906:127–134. [PubMed: 11430869]

Carter LM, Starkey ML, Akrimi SF, Davies M, McMahon SB, Bradbury EJ. The yellow fluorescent protein (YFP-H) mouse reveals neuroprotection as a novel mechanism underlying chondroitinase ABC-mediated repair after spinal cord injury. J Neurosci. 2008; 28:14107–14120. [PubMed: 19109493]

Chomsung RD, Petry HM, Bickford ME. Ultrastructural examination of diffuse and specific tectopulvinar projections in the tree shrew. J Comp Neurol. 2008; 510:24–46. [PubMed: 18615501]

Crawley AP, Jurkiewicz MT, Yim A, Heyn S, Verrier MC, Fehlings MG, Mikulis DJ. Absence of localized grey matter volume changes in the motor cortex following spinal cord injury. Brain Res. 2004; 1028:19–25. [PubMed: 15518637]

Feringa ER, Vahlsing HL. Labeled corticospinal neurons one year after spinal cord transection. Neurosci Lett. 1985; 58:283–286. [PubMed: 4047489]

Feringa ER, Vahlsing HL, Smith BE. Retrograde transport in corticospinal neurons after spinal cord transection. Neurology. 1983; 33:478–482. [PubMed: 6682195]

Ganchrow D, Bernstein JJ. Thoracic dorsal funicular lesions affect the bouton patterns on, and diameters of, layer VB pyramidal cell somata in rat hindlimb cortex. J Neurosci Res. 1985; 14:71–81. [PubMed: 4020899]

Gavrieli Y, Sherman Y, Ben-Sasson SA. Identification of programmed cell death in situ via specific labeling of nuclear DNA fragmentation. J Cell Biol. 1992; 119:493–501. [PubMed: 1400587]

Giehl KM, Tetzlaff W. BDNF and NT-3, but not NGF, prevent axotomy-induced death of rat corticospinal neurons in vivo. Eur J Neurosci. 1996; 8:1167–1175. [PubMed: 8752586]

Gundersen HJ. The nucleator. J Microsc. 1988; 151:3–21. [PubMed: 3193456]

Hains BC, Black JA, Waxman SG. Primary cortical motor neurons undergo apoptosis after axotomizing spinal cord injury. J Comp Neurol. 2003; 462:328–341. [PubMed: 12794736]

Hammond EN, Tetzlaff W, Mestres P, Giehl KM. BDNF, but not NT-3, promotes long-term survival of axotomized adult rat corticospinal neurons in vivo. Neuroreport. 1999; 10:2671–2675. [PubMed: 10574390]

Higo N, Nishimura Y, Murata Y, Oishi T, Yoshino-Saito K, Takahashi M, Tsuboi F, Isa T. Increased expression of the growth-associated protein 43 gene in the sensorimotor cortex of the macaque monkey after lesioning the lateral corticospinal tract. J Comp Neurol. 2009; 516:493–506. [PubMed: 19672995]

Holmes G, May WP. On the exact origin of the pyramidal tract in man and other mammals. Brain. 1909; 32:1–43.

Isenmann S, Wahl C, Krajewski S, Reed JC, Bahr M. Up-regulation of Bax protein in degenerating retinal ganglion cells precedes apoptotic cell death after optic nerve lesion in the rat. Eur J Neurosci. 1997; 9:1763–1772. [PubMed: 9283831]

Jurkiewicz MT, Mikulis DJ, McIlroy WE, Fehlings MG, Verrier MC. Sensorimotor cortical plasticity during recovery following spinal cord injury: a longitudinal fMRI study. Neurorehabil Neural Repair. 2007; 21:527–538. [PubMed: 17507643]

Kalil K, Schneider GE. Retrograde cortical and axonal changes following lesions of the pyramidal tract. Brain Res. 1975; 89:15–27. [PubMed: 1148840]

Klapka N, Hermanns S, Straten G, Masanneck C, Duis S, Hamers FP, Muller D, Zuschratter W, Muller HW. Suppression of fibrous scarring in spinal cord injury of rat promotes long-distance regeneration of corticospinal tract axons, rescue of primary motoneurons in somatosensory cortex and significant functional recovery. Eur J Neurosci. 2005; 22:3047–3058. [PubMed: 16367771]

Kost-Mikucki SA, Oblinger MM. Changes in glial fibrillary acidic protein mRNA expression after corticospinal axotomy in the adult hamster. J Neurosci Res. 1991; 28:182–191. [PubMed: 2033647]

Kost SA, Oblinger MM. Immature corticospinal neurons respond to axotomy with changes in tubulin gene expression. Brain Res Bull. 1993; 30:469–475. [PubMed: 8457896]

Kuypers, HGJM. In: The Nervous System, Handbook of Physiology. Vol. 2. Baltimore: Williams and Wilkins. Baltimore: Williams & Wilkins: 1981. Anatomy of the descending pathways; p. 597-666.

Kwon BK, Liu J, Messerer C, Kobayashi NR, McGraw J, Oschipok L, Tetzlaff W. Survival and regeneration of rubrospinal neurons 1 year after spinal cord injury. Proc Natl Acad Sci U S A. 2002; 99:3246–3251. [PubMed: 11867727]

Kwon BK, Liu J, Lam C, Plunet W, Oschipok LW, Hauswirth W, Di Polo A, Blesch A, Tetzlaff W. Brain-derived neurotrophic factor gene transfer with adeno-associated viral and lentiviral vectors prevents rubrospinal neuronal atrophy and stimulates regeneration-associated gene expression after acute cervical spinal cord injury. Spine. 2007; 32:1164–1173. [PubMed: 17495772]

Lassek AM. The pyramidal tract: a study of retrograde degeneration in the monkey. Arch Neurol Psychiatr (Chicago). 1942; 48:561–567.

Lee BH, Lee KH, Kim UJ, Yoon DH, Sohn JH, Choi SS, Yi IG, Park YG. Injury in the spinal cord may produce cell death in the brain. Brain Res. 2004; 1020:37–44. [PubMed: 15312785]

Lee SB, Beak SK, Park SH, Waterhouse BD, Lee HS. Collateral projection from the locus coeruleus to whisker-related sensory and motor brain regions of the rat. J Comp Neurol. 2009; 514:387–402. [PubMed: 19330821]

Levin PM, Bradford FK. The exact origin of the corticospinal tract in the monkey. J Comp Neurol. 1938; 68:411–422.

Maier IC, Baumann K, Thallmair M, Weinmann O, Scholl J, Schwab ME. Constraint-induced movement therapy in the adult rat after unilateral corticospinal tract injury. J Neurosci. 2008; 28:9386–9403. [PubMed: 18799672]

Martin WJ, Liu H, Wang H, Malmberg AB, Basbaum AI. Inflammation-induced up-regulation of protein kinase Cgamma immunoreactivity in rat spinal cord correlates with enhanced nociceptive processing. Neuroscience. 1999; 88:1267–1274. [PubMed: 10336135]

Mason MR, Lieberman AR, Anderson PN. Corticospinal neurons up-regulate a range of growth-associated genes following intracortical, but not spinal, axotomy. Eur J Neurosci. 2003; 18:789–802. [PubMed: 12925005]

Masterson SP, Li J, Bickford ME. Synaptic organization of the tectorecipient zone of the rat lateral posterior nucleus. J Comp Neurol. 2009; 515:647–663. [PubMed: 19496169]

McBride RL, Feringa ER, Garver MK, Williams JK Jr. Retrograde transport of fluoro-gold in corticospinal and rubrospinal neurons 10 and 20 weeks after T-9 spinal cord transection. Exp Neurol. 1990; 108:83–85. [PubMed: 1690666]

Merline M, Kalil K. Cell death of corticospinal neurons is induced by axotomy before but not after innervation of spinal targets. J Comp Neurol. 1990; 296:506–516. [PubMed: 2358550]

Migheli A, Attanasio A, Schiffer D. Ultrastructural detection of DNA strand breaks in apoptotic neural cells by in situ end-labelling techniques. J Pathol. 1995; 176:27–35. [PubMed: 7542332]

Mikucki SA, Oblinger MM. Corticospinal neurons exhibit a novel pattern of cytoskeletal gene expression after injury. J Neurosci Res. 1991; 30:213–225. [PubMed: 1724469]

Mikulis DJ, Jurkiewicz MT, McIlroy WE, Staines WR, Rickards L, Kalsi-Ryan S, Crawley AP, Fehlings MG, Verrier MC. Adaptation in the motor cortex following cervical spinal cord injury. Neurology. 2002; 58:794–801. [PubMed: 11889245]

Miller MW. The origin of corticospinal projection neurons in rat. Exp Brain Res Exp Hirnforsch. 1987; 67:339–351.

Mori M, Kose A, Tsujino T, Tanaka C. Immunocytochemical localization of protein kinase C subspecies in the rat spinal cord: light and electron microscopic study. J Comp Neurol. 1990; 299:167–177. [PubMed: 2229477]

Neumann S, Braz JM, Skinner K, Llewellyn-Smith IJ, Basbaum AI. Innocuous, not noxious, input activates PKCgamma interneurons of the spinal dorsal horn via myelinated afferent fibers. J Neurosci. 2008; 28:7936–7944. [PubMed: 18685019]

Nielson JL, Sears-Kraxberger I, Strong MK, Wong JK, Willenberg R, Steward O. Unexpected survival of neurons of origin of the pyramidal tract after spinal cord injury. J Neurosci. 2010; 30:11516–11528. [PubMed: 20739574]

NINDS. [Accessed April 16, 2010] National Institute of Neurological Disorders and Stroke. Facilities of Research Excellence in Spinal Cord Injury (FORE-SCI). 2008. Available at: http://www.ninds.nih.gov/funding/areas/repair_and_plasticity/fore_sci.htm

Ozden S, Isenmann S. Neuroprotective properties of different anesthetics on axotomized rat retinal ganglion cells in vivo. J Neurotrauma. 2004; 21:73–82. [PubMed: 14987467]

Paxinos, GW. The rat brain in stereotaxic coordinates. San Diego: Academic Press; 1998.

Piecharka DM, Kleim JA, Whishaw IQ. Limits on recovery in the corticospinal tract of the rat: partial lesions impair skilled reaching and the topographic representation of the forelimb in motor cortex. Brain Res Bull. 2005; 66:203–211. [PubMed: 16023917]

Pinzon A, Marcillo A, Quintana A, Stamler S, Bunge MB, Bram-lett HM, Dietrich WD. A re-assessment of minocycline as a neuroprotective agent in a rat spinal cord contusion model. Brain Res. 2008; 1243:146–151. [PubMed: 18838063]

Pisa M, Sanberg PR, Corcoran ME, Fibiger HC. Spontaneously recurrent seizures after intracerebral injections of kainic acid in rat: a possible model of human temporal lobe epilepsy. Brain Res. 1980; 200:481–487. [PubMed: 7417826]

Porter, R.; Lemon, R. Corticospinal function and voluntary movement. In: CAR, Boyd; AG, Brown; G, Fink; JS, Gillespie; C, Kidd; CC, Michell, editors. In: Corticospinal function and voluntary movement. Oxford: Clarendon Press; 1993.

Racine RJ. Modification of seizure activity by electrical stimulation. II. Motor seizure. Electroencephalograph Clin europhysiol. 1972; 32:281–294.

Ramirez LF, Kalil K. Critical stages for growth in the development of cortical neurons. J Comp Neurol. 1985; 237:506–518. [PubMed: 4044897]

Rosenzweig ES, Courtine G, Jindrich DL, Brock JH, Ferguson AR, Strand SC, Nout YS, Roy RR, Miller DM, Beattie MS, Havton LA, Bresnahan JC, Edgerton VR, Tuszynski MH. Extensive spontaneous plasticity of corticospinal projections after primate spinal cord injury. Nat Neurosci. 2010; 13:1505–1510. [PubMed: 21076427]

Rossi GF, Brodal A. Corticofugal fibres to the brain-stem reticular formation; an experimental study in the cat. J Anat. 1956; 90:42–62. [PubMed: 13295151]

Sasaki M, Hains BC, Lankford KL, Waxman SG, Kocsis JD. Protection of corticospinal tract neurons after dorsal spinal cord transection and engraftment of olfactory ensheathing cells. Glia. 2006; 53:352–359. [PubMed: 16288464]

Sasaki M, Radtke C, Tan AM, Zhao P, Hamada H, Houkin K, Honmou O, Kocsis JD. BDNF-hypersecreting human mesenchymal stem cells promote functional recovery, axonal sprouting, and protection of corticospinal neurons after spinal cord injury. J Neurosci. 2009; 29:14932–14941. [PubMed: 19940189]

Schmidlin E, Wannier T, Bloch J, Rouiller EM. Progressive plastic changes in the hand representation of the primary motor cortex parallel incomplete recovery from a unilateral section of the corticospinal tract at cervical level in monkeys. Brain Res. 2004; 1017:172–183. [PubMed: 15261113]

Schmidlin E, Wannier T, Bloch J, Belhaj-Saif A, Wyss AF, Rouiller EM. Reduction of the hand representation in the ipsilateral primary motor cortex following unilateral section of the corticospinal tract at cervical level in monkeys. BMC Neurosci. 2005; 6:56. [PubMed: 16135243]

Shinoda Y, Yamaguchi T, Futami T. Multiple axon collaterals of single corticospinal axons in the cat spinal cord. J Neurophysiol. 1986; 55:425–448. [PubMed: 3514812]

Sperk G, Lassmann H, Baran H, Kish SJ, Seitelberger F, Hornykiewicz O. Kainic acid induced seizures: neurochemical and histopathological changes. Neuroscience. 1983; 10:1301–1315. [PubMed: 6141539]

Starkey ML, Barritt AW, Yip PK, Davies M, Hamers FP, McMahon SB, Bradbury EJ. Assessing behavioural function following a pyramidotomy lesion of the corticospinal tract in adult mice. Exp Neurol. 2005; 195:524–539. [PubMed: 16051217]

Steward O, Sharp K, Selvan G, Hadden A, Hofstadter M, Au E, Ros-kams J. A re-assessment of the consequences of delayed transplantation of olfactory lamina propria following complete spinal cord transection in rats. Exp Neurol. 2006; 198:483–499. [PubMed: 16494866]

Steward O, Sharp K, Yee KM, Hofstadter M. A re-assessment of the effects of a Nogo-66 receptor antagonist on regenerative growth of axons and locomotor recovery after spinal cord injury in mice. Exp Neurol. 2008; 209:446–468. [PubMed: 18234196]

Thuret S, Moon LD, Gage FH. Therapeutic interventions after spinal cord injury. Nat Rev. 2006; 7:628–643.

Tseng GF, Prince DA. Structural and functional alterations in rat corticospinal neurons after axotomy. J Neurophysiol. 1996; 75:248–267. [PubMed: 8822555]

Walker NI, Harmon BV, Gobe GC, Kerr JF. Patterns of cell death. Methods Achieve Exp Pathol. 1988; 13:18–54.

Wannier T, Schmidlin E, Bloch J, Rouiller EM. A unilateral section of the corticospinal tract at cervical level in primate does not lead to measurable cell loss in motor cortex. J Neurotrauma. 2005; 22:703–717. [PubMed: 15941378]

Wrigley PJ, Gustin SM, Macey PM, Nash PG, Gandevia SC, Macefield VG, Siddall PJ, Henderson LA. Anatomical changes in human motor cortex and motor pathways following complete thoracic spinal cord injury. Cereb Cortex. 2009; 19:224–232. [PubMed: 18483004]

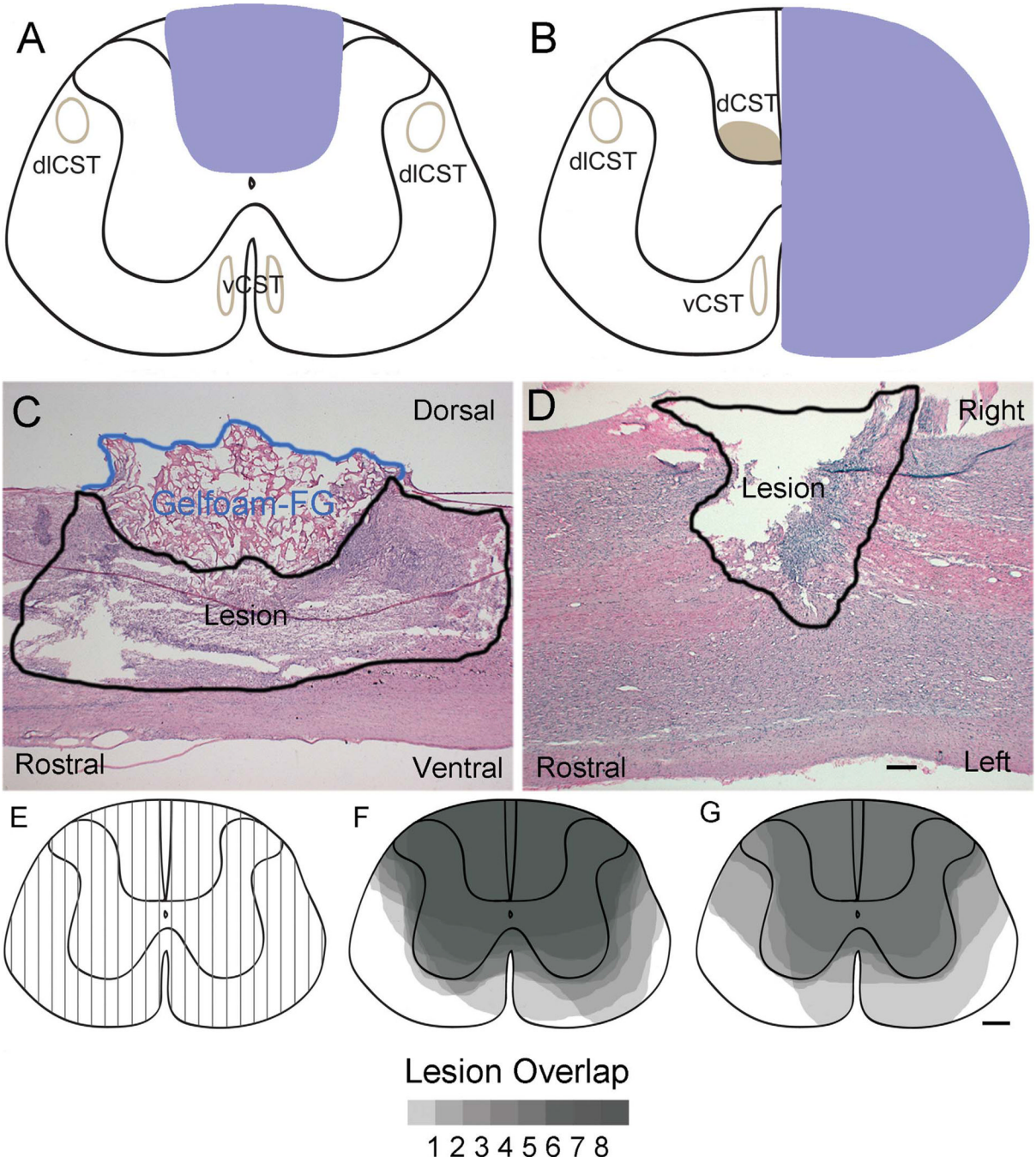

Figure 1.

Lesion verification. **A,B**: Schematic diagrams of the targeted lesion area for T9 dorsal funiculus (DF; A) and C5 hemisection (Hx; B) injuries. **C,D**: Representative hematoxylin and eosin (H&E)-stained sections for T9 DF (C) and C5 Hx injuries (D) for sagittal and horizontal sections, respectively. The area outlined in blue in C dorsal to the T9 DF lesion is the gelfoam that was impregnated with Fluoro-Gold (FG) and placed into the injury site. **E**: Lesion reconstruction technique for assessing sagittal sections for T9 DF lesions at 100-μm intervals throughout the injury site. **F,G**: The dorsoventral extent of the lesion in each sagittal section was represented on a schematic cross section for cases at 1 week (F) and 4

weeks (G) following injury. The gray scale illustrates areas of overlap of lesions in the different cases, with darkest areas indicating the regions of complete overlap. dlCST, dorsolateral corticospinal tract; dCST, dorsal CST; vCST, ventral CST. Scale bar = 500 μm in D (applies to C,D); 200 μm in G (applies to E–G).

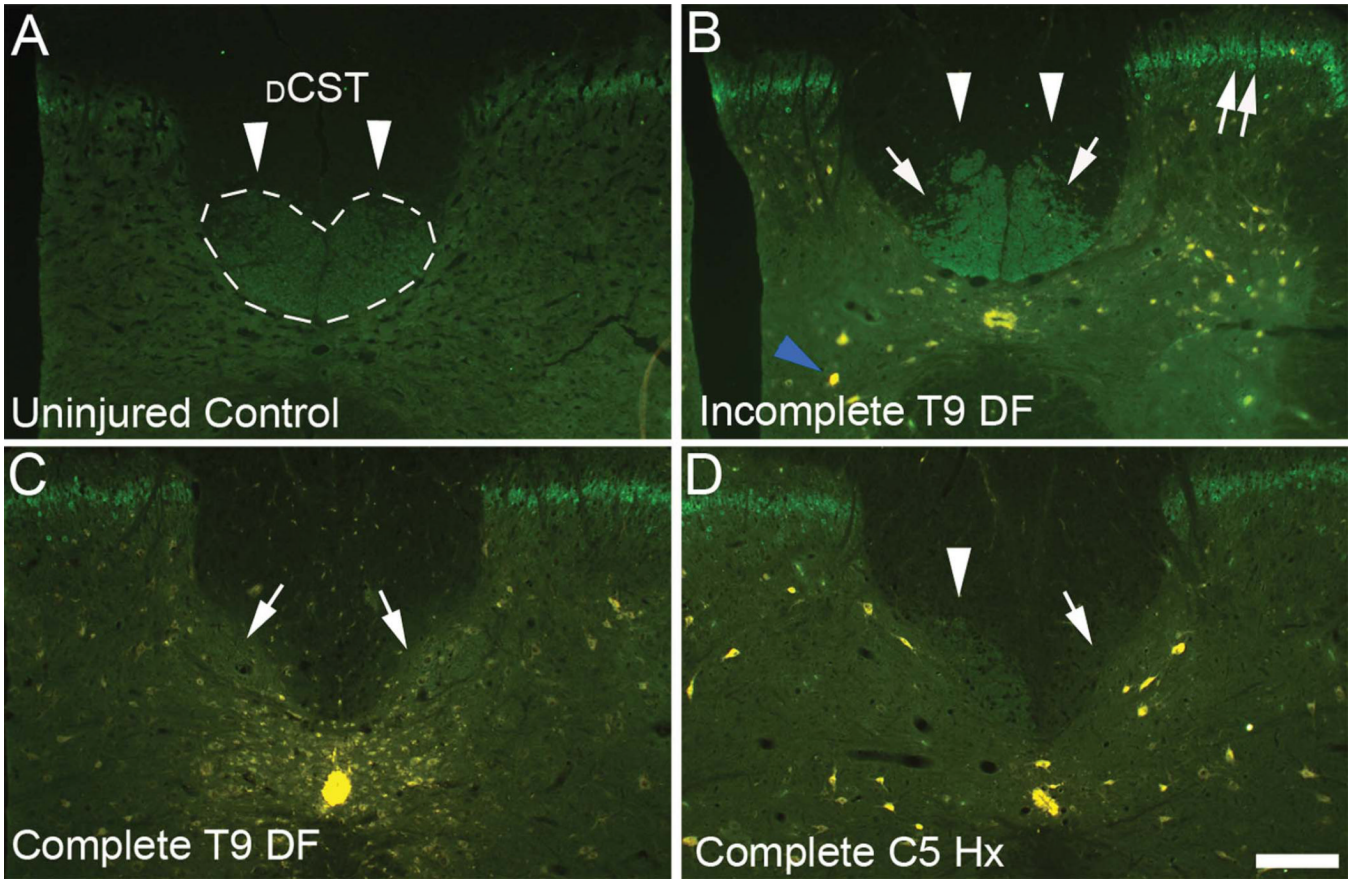

Figure 2.

Assessment of spared CST fibers caudal to the lesion by immunostaining for PKCγ. **A**: In uninjured control rats, CST axons in the dorsal column stain positively for PKCγ (arrowheads). The dorsal CST (dCST) is outlined in dashed lines. **B**: In animals with incomplete lesions, immunostaining is preserved in part of the distribution of CST axons (arrowheads). Arrows indicate areas in which staining is eliminated due to degeneration of CST axons. **C**: In rats with complete DF lesions, immunostaining for PKCγ is eliminated in the area of the dCST (arrows). **D**: In rats with complete hemisections, spared CST axons stain for PKCγ on the side contralateral to the lesion (arrowheads) but immunostaining is eliminated on the side of the lesion (arrows). Note also increased immunostaining of interneurons in lamina II of the dorsal horn (double arrows). Additionally, residual Fluoro-Gold (FG) labeling can be seen in the central canal and in cells in the gray matter (blue arrowhead). Scale bar = 200 μm in D (applies to A–D).

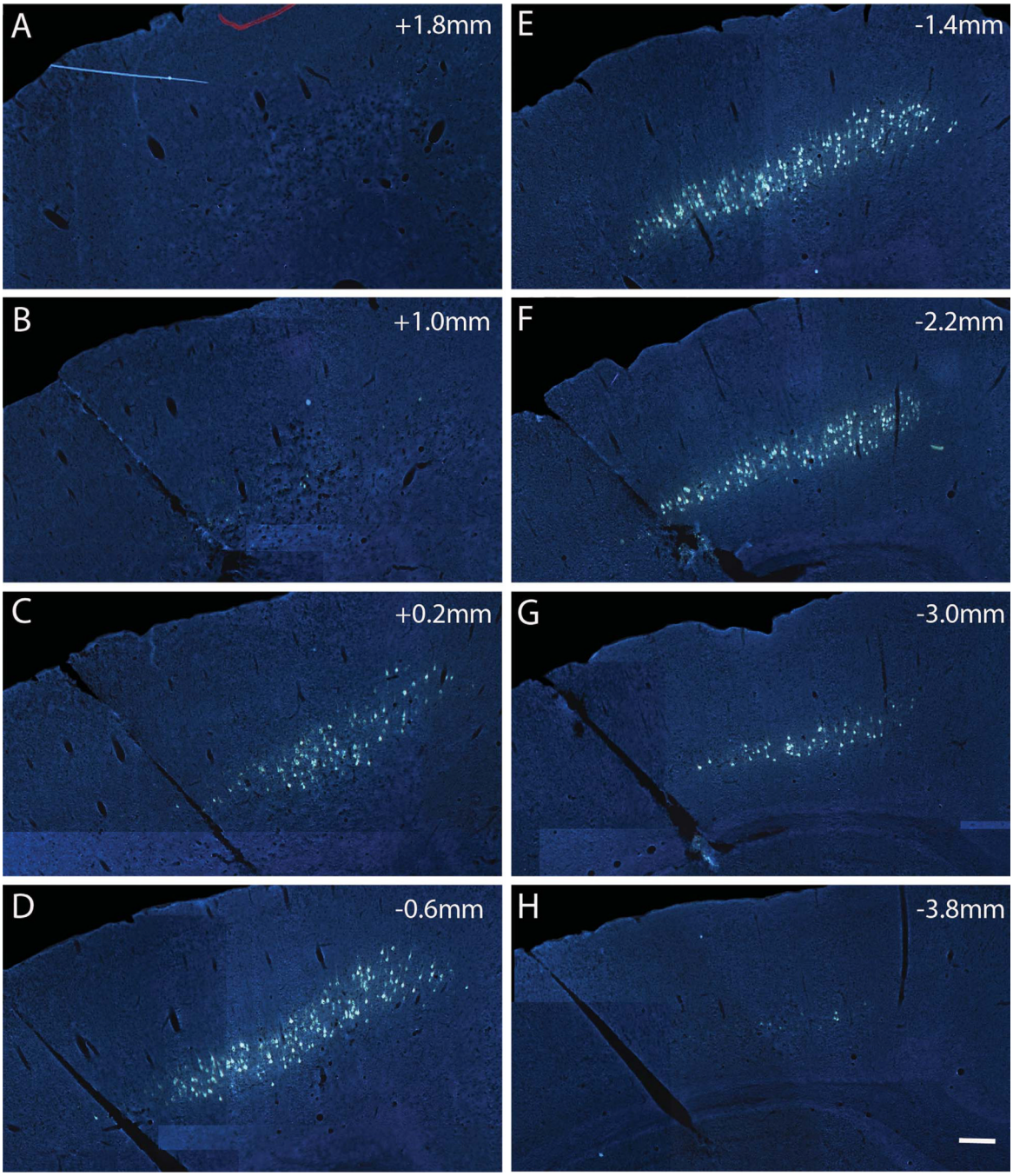

Figure 3.

Rostrocaudal distribution of FG-labeled CST cell bodies with FG/gelfoam implants into lesion sites at T9. **A–H**: Distribution of retrogradely labeled cells in layer V of the left sensorimotor cortex in a rat with an FG implant at the T9 dorsal funiculus (DF) injury site. Labeling spans from 1.8 mm (rostral, A) to −3.8 mm (caudal, H) from Bregma 1 week following injury and labeling. Scale bar = 500 μm in H (applies to A–H).

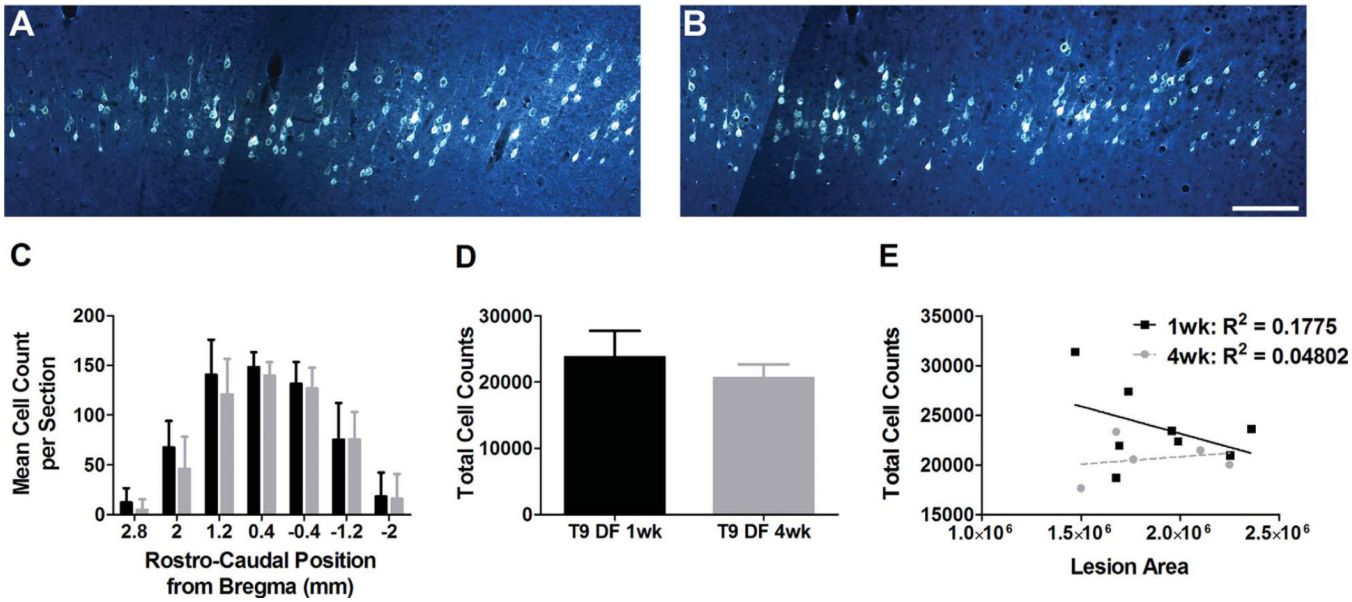

Figure 4.

Quantification of FG-labeled CST cell bodies following SCI. **A**: Fluoro-Gold (FG)-labeled cells in the cortex 1 week following T9 DF lesion. **B**: FG-labeled cells in the cortex 4 weeks following T9 DF lesion. **C**: Stereological quantification of FG retrogradely labeled cells rostrocaudally in the cortex 1 and 4 weeks following T9 DF lesions. **D**: Total cell counts throughout the cortex 1 and 4 weeks following T9 DF lesions, based on stereological quantification of FG-labeled cells. **E**: No correlation between total cell counts and lesion area 1 and 4 weeks following T9 DF lesions. Data are mean ± SD. Scale bar = 200 μm in B (applies to A,B).

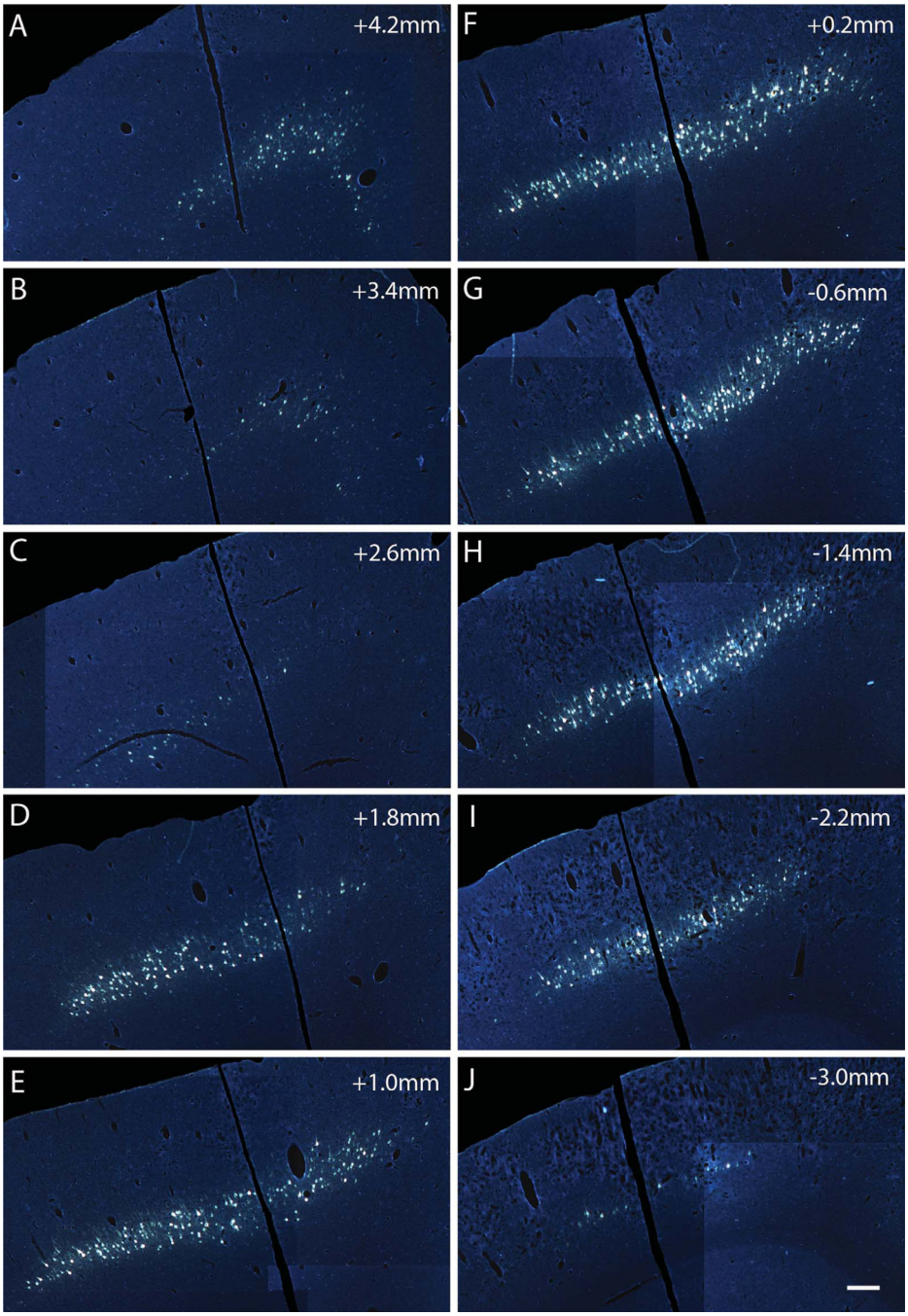

Figure 5.

Rostrocaudal distribution of FG-labeled CST cell bodies with FG/gelfoam implants into lesion sites at C5. **A–J**: Distribution of retrogradely labeled cells in layer V of the left sensorimotor cortex in a rat with an FG implant at the C5 hemisection (Hx) site. Labeling spans from 4.2 mm (rostral, A) to −3.8 mm (caudal, J) from Bregma 1 week following injury and labeling. Scale bar = 500 μm in J (applies to A–J).

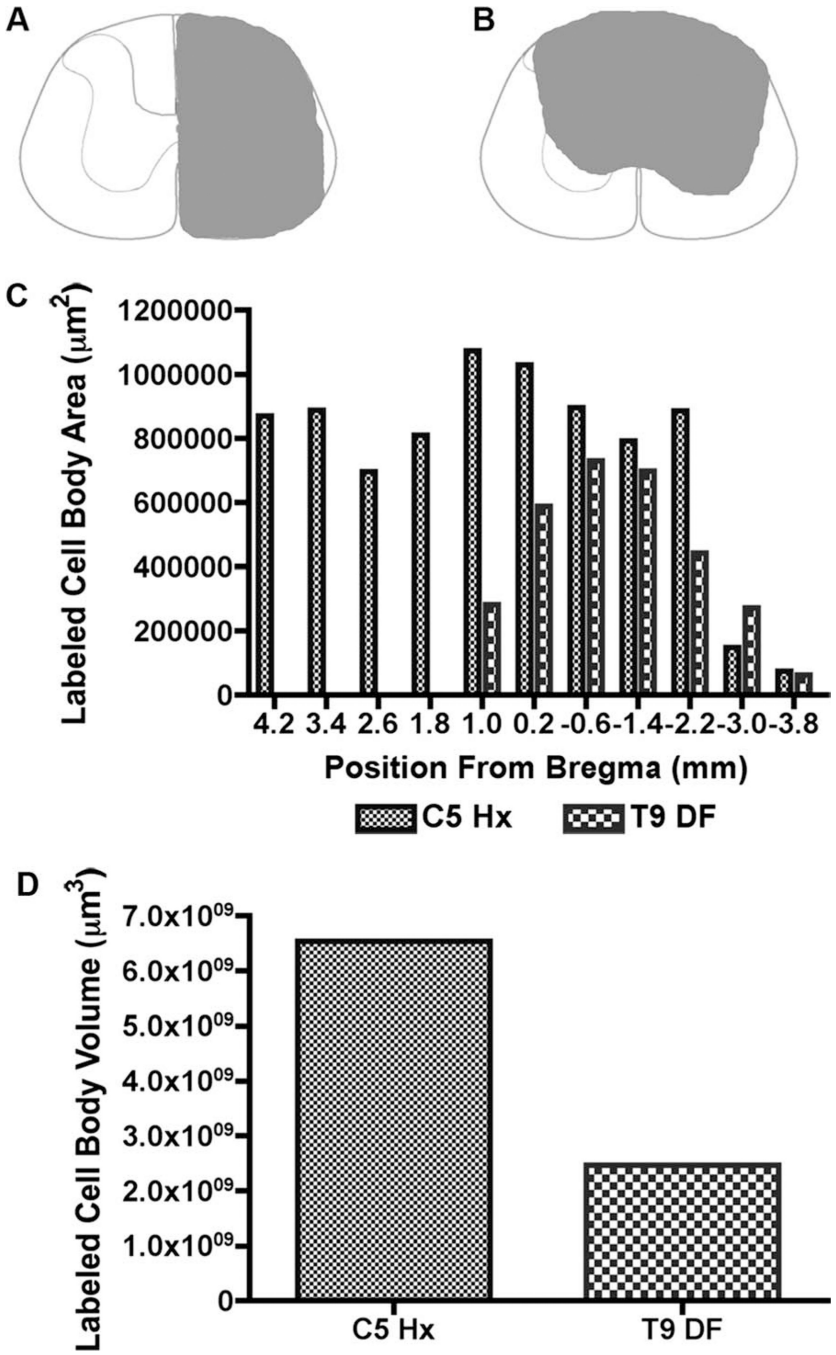

Figure 6.

Area and volume measurements of FG-labeled CST cell bodies with FG/gelfoam implants into lesion sites at C5 and T9. **A**: Lesion reconstruction of C5 Hx. **B**: Lesion reconstruction of T9 DF. **C**: Distribution of retrogradely labeled cell bodies throughout the cortex 1 week following C5 hemisection (Hx) and T9 dorsal funiculus (DF) lesions. **D**: Estimated volume of the cortex containing retrogradely labeled cells 1 week following C5 Hx and T9 DF.

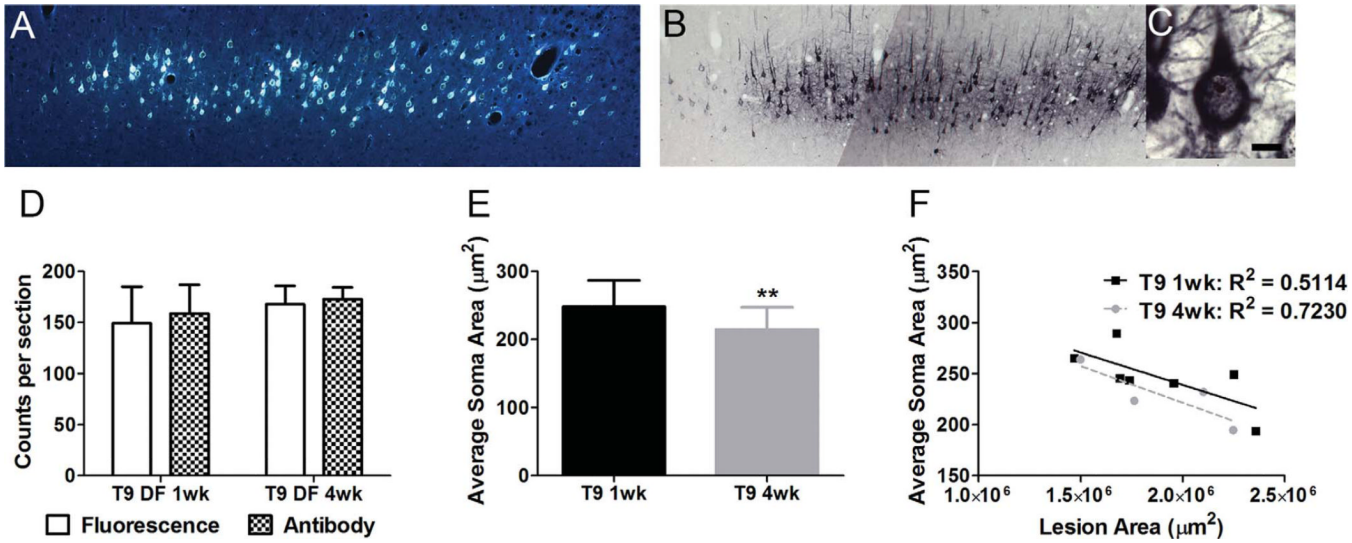

Figure 7.

Evidence for retrograde atrophy following SCI. **A**: FG fluorescence in layer V of the cortex following labeling at T9. **B,C**: FG detection following immunohistochemistry with an antibody to FG following labeling at T9 (B), and an example of a prominent nucleolus (C) used to assess cell sizes for atrophy. **D**: Quantification of FG-labeled cells showing no difference between detecting FG with fluorescence or the antibody. **E**: Average cell size/area of FG-labeled cells shows significant decreases in soma area between 1 (black column) and 4 weeks (gray column) following a T9 DF lesion. **F**: Despite variability in lesion size, there is no significant correlation between lesion size and cell size following T9 DF lesions. Data are mean ± SD; **, $P < 0.01$. Scale bar = 10 μm in C (applies to C).

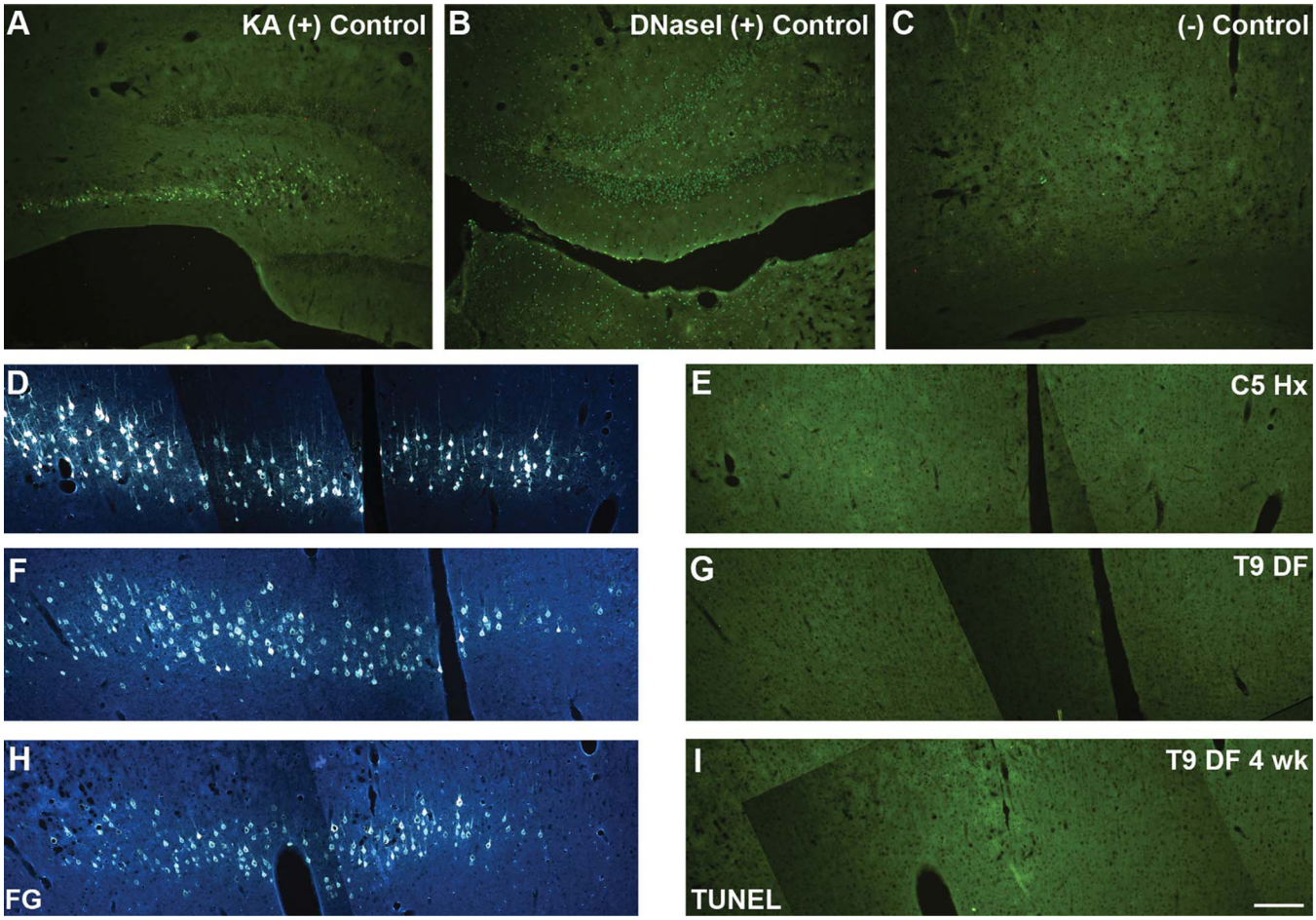

Figure 8.

No evidence for apoptosis of axotomized cortical motoneurons as assessed by TUNEL staining. **A**: Positive control for TUNEL staining reveals neurons undergoing excitotoxic cell death in the hippocampus after kainic acid (KA)-induced status epilepticus. **B**: TUNEL staining after DNAse treatment (another positive control for TUNEL staining). **C**: A negative control in which the tissue was processed alongside the positive controls and sample tissue, without addition of the TdT enzyme. **D,F,H**: Retrogradely labeled neurons 1 week following either a C5 hemisection (Hx) (D) or a T9 dorsal funiculus (DF) lesion (F), or 4 weeks following a T9 DF lesion (H). **E,G,I**: TUNEL-stained sections in the region containing FG-labeled cells 1 week following C5 Hx (E), T9 DF lesion (G) or 4 weeks following T9 DF (I). Note complete absence of TUNEL-stained cell bodies in cases with spinal cord injuries. Scale bar = 200 μm in I (applies to A–I).

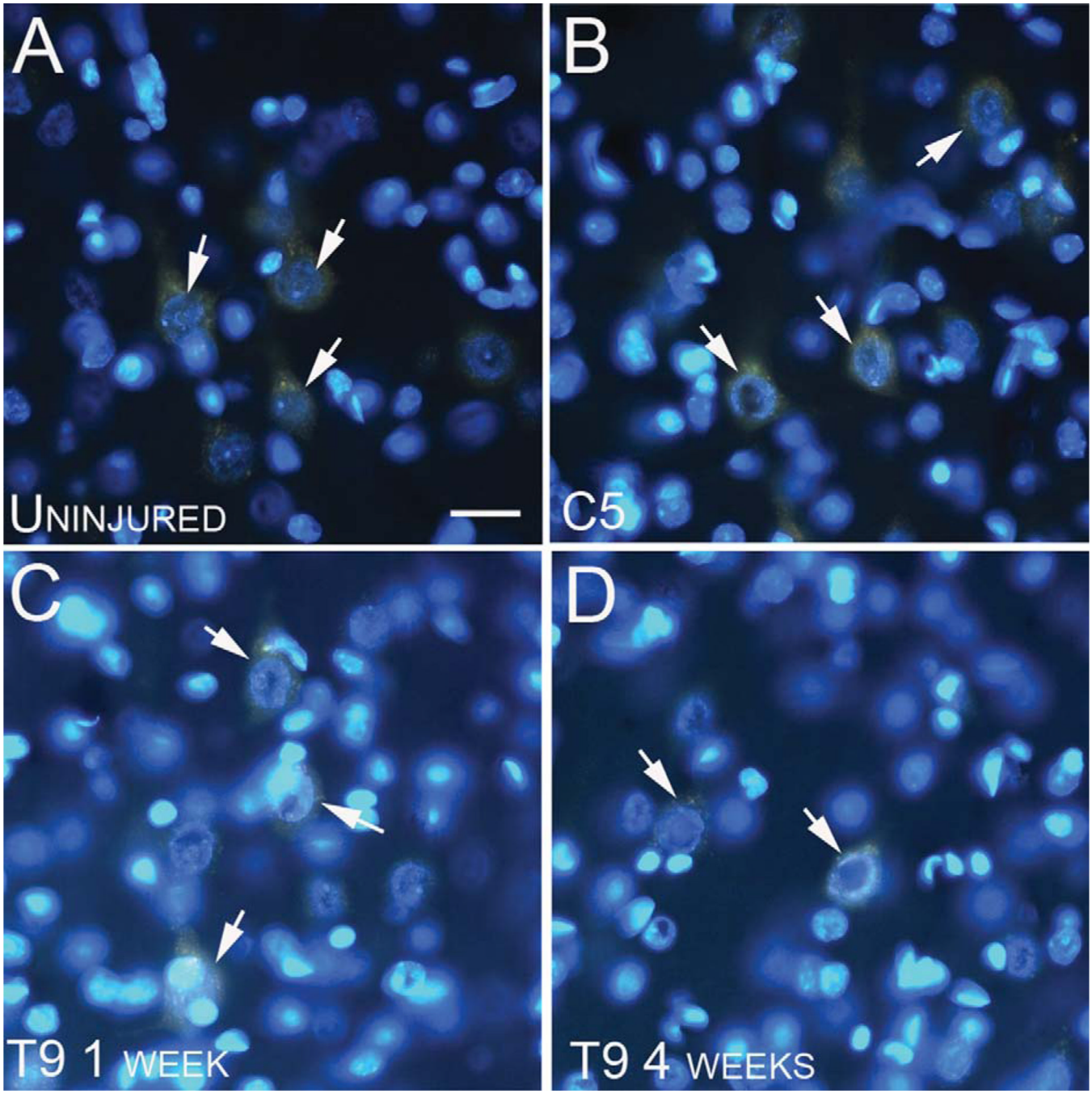

Figure 9.

No morphological evidence of nuclear abnormalities in retrogradely labeled CST cell bodies following SCI. **A–D**: Fluorescence micrographs illustrating CST cell bodies labeled with Fluoro-Gold (orange), displaying healthy nuclei stained with Hoechst (blue) in uninjured (A), C5 hemisection at 1 week (B), T9 dorsal funiculus (DF) lesion at 1 week (C), and T9 DF at 4 weeks (D) post injury. All cells show nuclei labeled within the cell body, and displaying healthy nucleoli (arrows). Scale bar = 40 μm in A (applies to A–D).

TABLE 1

Primary Antibodies Used in This Study

Antigen	Dilution	Host Species	Source	Catalogue No.	Immunogen
PKCγ	1:500	Rabbit	Santa Cruz Biotechnology, Santa Cruz, CA	sc-211, lot #E-10-10	Amino acid residues 679–697 of mouse PKCγ (DFVHPDARSPTSPVPVPVM)
FG	1:60,000	Rabbit	Fluorochrome, Denver, CO	Antibody to FG, lot #1-7-09	Fluoro-Gold

PKCγ, polyclonal antibody to the γ subunit of protein kinase C; FG, polyclonal antibody to Fluoro-Gold (FG).